Borromean hypergraph formation in dense random rectangles

Alexander R. Klotz
Department of Physics and Astronomy, California State University, Long Beach, 1250 Bellflower Boulevard, California 90840, USA

(Received 31 May 2024; accepted 16 August 2024; published 6 September 2024)

We develop a minimal model to study the stochastic formation of Borromean links within topologically entangled networks without requiring the use of knot invariants. Borromean linkages may form in entangled solutions of open polymer chains or in Olympic gel systems such as kinetoplast DNA, but it is challenging to investigate this due to the difficulty of computing three-body link invariants. Here, we investigate rectangles randomly oriented in three Cartesian planes and densely packed within a volume, and evaluate them for Hopf linking and Borromean link formation. We show that dense packings of rectangles can form Borromean triplets and larger clusters, and that in high enough density the combination of Hopf and Borromean linking can create a percolating hypergraph through the network. We present data for the percolation threshold of Borromean hypergraphs, and discuss implications for the existence of Borromean connectivity within kinetoplast DNA.

DOI: 10.1103/PhysRevE.110.034501

I. INTRODUCTION

The physical properties of a soft filamentous system are dictated by the degree of entanglement between its constituents [1]. Examples include the viscoelasticity induced by entanglements in polymer melts [2], the tangling and untangling dynamics of living worms [3], and the elastic curvature of kinetoplast DNA (kDNA) networks [4]. Traditionally, entanglement between two filaments may be described the by Gauss linking number, which describes the integer number of times two closed curves pass through each other, and can be generalized to the real number of times two open curves intertwine [5]. Certain materials share exotic entanglements that cannot be described by the linking number. For example, dense solutions of ring polymers contain interpenetrations of closed loops that affect the viscoelastic properties of the system [6], and so-called daisy chains may be formed of unlinked but deadlocked rings [7], which cannot be separated by stretching the system. Another exotic form of entanglement is Borromean rings, which consist of three topologically connected loops in which no two share a direct topological link [Fig. 1(a)]. These three-body links cannot be detected by the Gauss linking number, which yields zero for each subset of two loops, but may be computed with more complex metrics such as the Milnor triple integral [8]. Densely entangled polymer networks may form open Borromean rings (similar to the strands in braided hair), and a limited number of simulation studies have detected them using the Jones [9] or HOMFLY polynomials [10]. Recently, Ubertini and Rosa simulated dense solutions of ring polymers in which the topology may evolve through Monte Carlo operations that pass parts of chains through each other and used the three-body Jones polynomial to show that triplets of loops may form Borromean rings [11]. Random Borromean entanglements have not been observed experimentally. Physical realizations of a randomly linked ring polymer system may include Olympic gels of circular DNA molecules facilitated by topoisomerase II enzymes, either naturally in the kinetoplast (the molecular chain-mail network found in the mitochondria of trypanosome parasites [12]) or *in vitro* [13,14]. Dense solutions of synthetic polymers in which cyclization reactions may occur can also yield randomly formed topological links. It is known that dense packings of rings [15] or ring polymers [16] may form a sufficient density of topological links that a single linked network may percolate across the system. This linking percolation transition has been investigated computationally in the context of kinetoplasts. It is unknown if entangled polymer solutions, kinetoplast networks, or DNA-based Olympic gels contain Borromean links, and this paper is motivated by the possibility of their existence.

Recently, we investigated the percolation transition in Borromean networks of loops on a square lattice, in which no two loops are linked but each triplet of neighbors is [17]. Whereas Hopf-linked networks may be described as graphs in which each loop is a node and each linked connection is an edge, Borromean networks must be described as hypergraphs, in which the interdependent connections of three loops define a triangle of edges and nodes. The removal of a node or edge from a triangular hypergraph destroys the remaining edges. We found that the percolation transition occurs at a slightly higher fraction of occupied sites than for a regularly

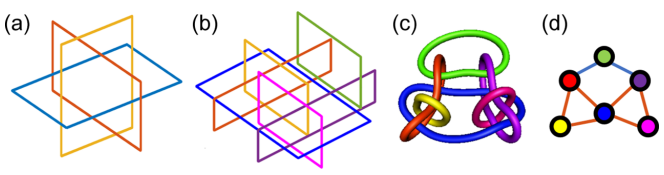

FIG. 1. (a) Borromean rings consisting of three perpendicular rectangles with a golden aspect ratio (1.618). (b) A network of six rectangles connected by both Hopf and Borromean linking. (c) The same network, with each component rendered as an elastic loop. (d) Hypergraph structure of the network, in which nodes sharing a Hopf link are connected with a blue edge, and each triplet of Borromean linked rings form a red triangle of edges.

linked network. It was subsequently proven by Bianconi and Dorogovtsev [18] that hypergraphs have a higher node percolation threshold than their graph counterparts in general. Our previous work exploited the regularity of the square lattice to study Borromean percolation, but for networks of randomly linked rings it is not known how likely the formation of Borromean components is, nor is it known whether Borromean networks can randomly form in the presence of regularly linked networks. For example, if given ring is linked with every other ring in its spatial vicinity, it will be unable to share Borromean connections. It is challenging to investigate this computationally due to the complexity of computing triple link invariants and the combinatoric challenge of three-ring interactions.

Here, we describe a minimal model with which to examine the coexistence of regular (Hopf) and Borromean linking. We study rectangles aligned with the three Cartesian planes randomly packed within a volume [Fig. 1(b)], which can be mapped onto a system of ring polymers [Fig. 1(c)]. We can determine Borromean linking by simple comparison of the rectangles' coordinates, and construct the (hyper)graph structure of the linkages that form [Fig. 1(d)]. This allows us to examine the possibility and probability of Borromean links and percolating clusters forming in dense random networks, suggesting analogous effects for more complex polymer systems.

II. METHODS

The model is initialized by placing rectangles in a cubic box according to a uniform random distribution in X, Y, and Z. The rectangles have a common aspect ratio that can be varied and a total area of 4. The number of rectangles N and the width of the box L can be varied to tune the number density. The box constrains the centers of each rectangle, such that their extrema may lie beyond the edge the box. The rectangles have random orientations aligned with the three Cartesian axes, such that each may lie parallel to the XY, YZ, or XZ planes with normal vectors in the Z, X, and Y directions, respectively. Each rectangle is randomly landscape or portrait, such that on average half the rectangles in each plane have a width exceeding their height and vice versa. Typical systems have N on the order of several hundred or thousand to initialize a dense random network of rectangles. To examine systems analogous to the quasi-two-dimensional (quasi-2D) kinetoplast networks, we can limit the translation distribution in one of the dimensions, and initialize their positions to uniformly fill a circle rather than a square or cube. After initializing the rectangles, we evaluate linking and network formation through methods described below.

Consider two rectangles lying in perpendicular planes. We may define rectangle A as lying in plane ij with a normal along k, and rectangle B lying in plane jk with a normal along i. The j direction is shared, i and k are unshared between the rectangles. We define the terms A_{i+} and A_{i-} as the maximum and minimum position of A along the i direction, and A_{k0} as the location of A along its normal direction. Similar terms can be defined for the other rectangle and directions. For two rectangles to have any sort of topological connection they must be collocated along their unshared axes, which is satisfied when:

$$A_{i-} < B_{i0} < A_{i+}$$
$$\text{and } B_{k-} < A_{k0} < B_{k+}.$$

If the rectangles are collocated in their unshared dimension, then they are Hopf linked if one maximum or minimum of a rectangle in the shared dimension lies between the maximum and minimum of the other rectangle, satisfying either of the two following sets of conditions:

$$A_{j-} < B_{j-} \ \& \ A_{j+} > B_{j-} \ \& \ A_{j+} < B_{j+}$$
$$\text{or } A_{j-} > B_{j-} \ \& \ A_{j-} < B_{j+} \ \& \ A_{j+} > B_{j+}.$$

Two rectangles can be unlinked, but one can be said to pierce another if they lie in different planes, are collocated in their unshared dimensions, and both extrema in the shared dimension of one rectangle lie between the extrema of the other. The conditions for A piercing B ($A \to B$) are

$$B_{j-} < A_{j-} \text{ and } B_{j+} > A_{j+}.$$

Unlike linking, piercing does not commute. If the inequalities are reversed, then we may say that $B \to A$. Three rectangles A, B, C with mutually perpendicular normals form a Borromean triplet if either of two conditions are met: either $A \to B \to C \to A$, or $A \to C \to B \to A$. In principle rectangles may intersect at points or overlap in the same plane, but in practice this is prevented by the precision of our random number generator.

To efficiently evaluate linking in the dense rectangular networks, we first check each pair of rectangles for collocation, then conditionally check Hopf linking, then conditionally check collocated unlinked rectangles for piercing. Sorting rectangles by their normal axis and prechecking each pair for collocation and linking before checking each triplet for piercing alleviates the cubic growth of the number of needed comparisons. For example, a system of 100 rectangles admits $\binom{100}{3} = 161\ 700$ triplets, but even in dense percolating networks only around 25 full three-rectangle piercing checks are required. Our scheme is considerably simpler than computing a knot invariant such as the Milnor triple linking integral or the Jones polynomial.

To generate a hypergraph representation of the rectangle packing, each pair of unique rectangles A and B is checked for Hopf linking; if two rectangles are linked then two bits, G_{AB} and G_{BA}, on a binary $N \times N$ graph adjacency matrix G are flipped. Then, each pair of unlinked normally perpendicular rectangles is checked for piercing, and if they are pierced then each rectangle C that is normally perpendicular to and unlinked with the other two is checked for piercing. If the three rectangles satisfy the Borromean conditions, six bits of a binary hypergraph adjacency matrix are flipped: H_{AB}, H_{AC}, H_{BC}, and their transpose partners. These two matrices are used to generate a graph structure using MATLAB's graph function, which converts a matrix to a table of nodes and edges that can be used to plot a graph visualization and determine the sizes of connected components using standard algorithms [19]. We track the size of the largest two components of G and H as a function of the number density of rectangles. The combined hypergraph is generated as $HG = 2H + G$, where

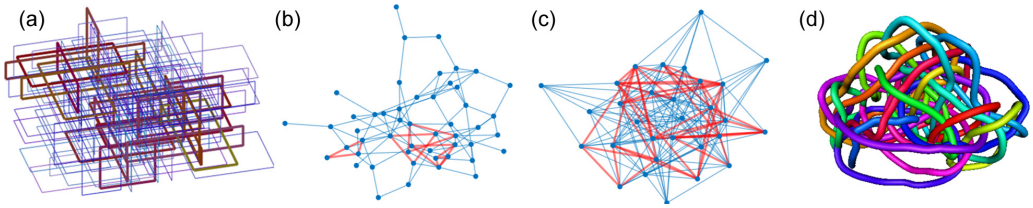

FIG. 2. (a) Random network of rectangles in which those participating in Borromean linking are highlighted. (b) A hypergraph structure in which Hopf linked rectangles (blue edges) have formed a percolating cluster and several Borromean components (red triangles) have formed. (c) A hypergraph structure in which both Hopf linked and Borromean linked rectangles have formed percolating clusters. (d) Rendering of the Borromean network in (c) as elastic loops.

the magnitude of each matrix site now contains information about the weight of each edge for visualization.

III. RESULTS AND DISCUSSION

This study was motivated by the question of whether Borromean links can form in dense randomly linked systems, and by extension whether these Borromean connections can create a percolating hypergraph. Simulations show that the answer to both these questions is yes. Figure 2(a) shows an example of a rectangle network, with rectangles that share Borromean connections highlighted. Figure 2(b) shows a hypergraph representation of a network with each node representing a rectangle, each blue edge representing a Hopf link, and each red triangle representing a Borromean triplet. In this case, the Hopf connections form a percolating cluster and a few Borromean components lie within it. Figure 2(c) shows a denser network in which the Borromean connections form a percolating cluster as well. The rectangles that form this percolating Borromean cluster are shown annealed and visualized as elastic filaments in Fig. 2(d), although it is difficult by eye to identify the connectivity.

We can examine the Hopf and Borromean percolation transitions by examining the size of the largest connected components as a function of the density of the rectangle packing. Although the density of two-dimensional objects in three-dimensional space is difficult to define, the number density $\rho = N/L^3$ (where L is the length of the box that constrains the centers of rectangles) allows data collapse for different numbers of rings. If all rectangles have a uniform size and aspect ratio, a dense packing creates two separate but interpenetrating Borromean networks in denser systems, one in which the XY rectangles are portrait and one in which they are landscape. This phenomenon is discussed in the Appendix. To track percolation in Borromean systems we examine the fraction of nodes that are in either of the two largest clusters, rather than just the largest. This is unnecessary if the rectangles are given a distribution of aspect ratios, even if the variation is limited to 10% of the aspect ratio. Since the percolation threshold depends on the specific value or distribution of aspect ratios and we are primarily concerned with whether percolation is possible, we do not seek a detailed measure of the percolation threshold through the entire parameter space or the critical exponents at percolation. We simply use linear interpolation to find the point at which the probability of a node being in the largest component reaches 50%.

Figure 3(a) shows the fraction of 500 rectangles that are found in the largest cluster or clusters, as a function of the number density. Aspect ratios between 1.25 and 10 were explored, and the area of the rectangles was held constant. As predicted by Bianconi and Dorogovtsev [18], the Borromean networks have a higher percolation threshold. The Borromean percolation threshold may be orders of magnitude higher in density than the Hopf linking threshold, in comparison to the 1.6% difference we observed in Borromean square lattices [17]. The critical densities at percolation for Hopf and Borromean networks are shown in Fig. 3(b), as well as data taken when the perimeter was held constant instead of the area. Interestingly, while the percolation threshold of Hopf linked networks appears to be independent of aspect ratio when the area is held constant, it decreases with aspect ratio for Borromean networks. There is an extremely weak but significant (-0.07 power) dependence on the Hopf critical density and this is believed to be a finite-size effect. When the perimeter is held constant, the Hopf linking percolation threshold increases with the aspect ratio, but the Borromean threshold is nonmonotonic, reaching a minimum at around 3. The ratio of the Borromean to Hopf thresholds is essentially the same between the area and perimeter data, and appears to approach an 8 : 1 ratio in density. The difference between constant area and constant perimeter may have to do with a subtle rescaling of the system's length scale when the aspect ratio is changed, affecting the definition of density. For overlapping randomly oriented rectangles in two dimensions, the percolation density also decreases with aspect ratio [20].

We can heuristically understand these results by considering two perpendicular congruent rectangles with orientations that allow piercing. Rectangle A in the XY plane has width a and height $b > a$, rectangle B is in the XZ plane with width b and height a. Both are contained within a box of side length L with $L \gg b$. The crux of the argument is that their range of overlap in the x direction depends on $a + b$, of which $2a$ of that range leads to linking and $b - a$ leads to piercing. If we fix the position of A and treat the location of B as variable, the probabilities that the collocation conditions are met are a/L in the z direction and b/L in the y direction such that:

$$P_C = \frac{ab}{L^2}.$$

If this is satisfied, we consider the relative x positions of A and B. In the notation above, $A_{j-} = A_{x-}$, $A_{j+} = A_{x-} + a$, $B_{j-} = B_{x-}$, and $B_{j+} = B_{j-} + b$, knowing that the right side of A is a from the left side, and the right side of B is b from the left

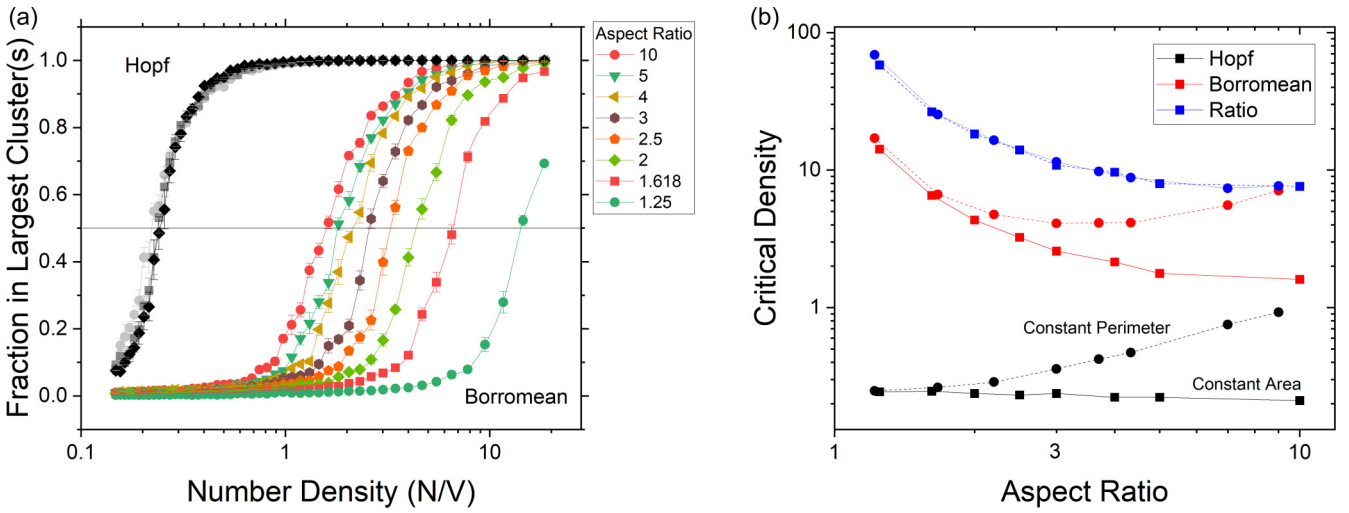

FIG. 3. (a) Percolation transition of dense rectangle networks as determined by the fraction of rectangles that are part of largest cluster (Hopf), or part of the largest two clusters (Borromean), as a function of the number density. Networks contained 500 rectangles with aspect ratios between 1.25 and 10. Three shown sets of Hopf data (1.25, 2, and 5) mostly overlap. The area of the rectangles was held constant as the aspect ratio was varied. (b) Approximate density at percolation for Hopf and Borromean networks as a function of the rectangular aspect ratio. The dimensionless ratio between the two densities is also shown. Data for constant area are shown with square points and continuous connectors, data for constant perimeter are shown with round points and dashed connectors.

side. The rectangles may be linked if the left side of B is within distance b left of the left side of A, and not beyond the right side of A ($B_{x-}+b>A_{x-}$, $B_{x-}<A_{x-}+a$). The total range that the left side of B has in order for an overlap to happen is $a+b$ and the probability is $(a+b)/L$. However, if both sides of A are within the x confines of B ($B_{x-}<A_{x-}$, $B_{x-}+b>A_{x-}+a$), they will pierce instead of link. The range of positions for B_{x-} in this case is $(b-a)$. The probability of linking and piercing given collocation are thus

$$P_{L|C}=\frac{b+a}{L}-\frac{b-a}{L}=\frac{2a}{L}\ \ \&\ \ P_{P|C}=\frac{b-a}{L}.$$

The total probabilities of two rectangles being linked or pierced is

$$P_L=\frac{2ba^2}{L^3}\ \ \&\ \ P_P=\frac{ab}{L^3}(b-a).$$

We can define the aspect ratio $\gamma=b/a$ and a density $\rho=(a/L)^3$ and rewrite these probabilities as

$$P_L=2\gamma\rho\ \ \&\ \ P_P=\gamma(\gamma-1)\rho.$$

Their ratio is

$$\frac{P_L}{P_C}=\frac{2\gamma}{\gamma(\gamma-1)}=\frac{2}{\gamma-1}.$$

This ratio reveals features of the topological probabilities in our rectangle system. As the aspect ratio approaches unity from the right, the ratio diverges, indicating that it is impossible to form a Borromean network with squares. Beyond an aspect ratio of 3, piercing becomes more likely than linking. The probability of three simultaneous Borromean piercings can be treated as the cube of the piercing probability. The probability has a cubic dependence on number density meaning that the link-to-Borromean ratio is not just a function of aspect ratio and decreases with the square of number density. This may explain the dramatic difference in density dependence between the Hopf and Borromean percolation thresholds. While an understanding of the linking and piercing probabilities of two rectangles is helpful in understanding the percolation data, we do not yet have a full derivation of the trends in Fig. 3.

Borromean links and percolating hypergraphs were also observed in quasi-2D networks, suggesting a possibility that kinetoplast networks may contain Borromean links. To estimate the number of Borromean links contained in a kinetoplast network, should they exist, we can simulate networks with thousands of components, comparable to kDNA, and tune the number density of rectangles such that the average number Hopf links per rectangle matches the average kDNA minicircle valence, approximately 3 [21,22]. From these networks we can compute the number of rectangles participating in Borromean linking, and the total number of Borromean clusters. Figure 4(a) shows an example hypergraph from a quasi-2D system of 3000 rectangles and an average Hopf valence of approximately 3. Several Borromean clusters are interspersed through the network, with several of larger examples shown in Fig. 4(b). The largest cluster contains 20 rectangles, but there are 87 Borromean triplets throughout the network. Note that the visualizations in Fig. 4(b) may have ambiguity in the total number of triangles each node belongs to.

The topology of kinetoplast DNA from *Crithidia fasciculata* is at this time the best characterized, and it contains approximately 5000 minicircles. We measure the total number of links that are part of a Borromean triplet or cluster, as well as the total number of Borromean clusters. The disk-shaped networks contained 5000 rectangles with an aspect ratio uniformly between 1.5 and 2.5, and had an effective thickness of 0.1, and were varied in radius to change the density. As the Borromean portion of the network approaches percolation, the number of involved rectangles increases while the number of clusters reaches a maximum before approaching 1. When the

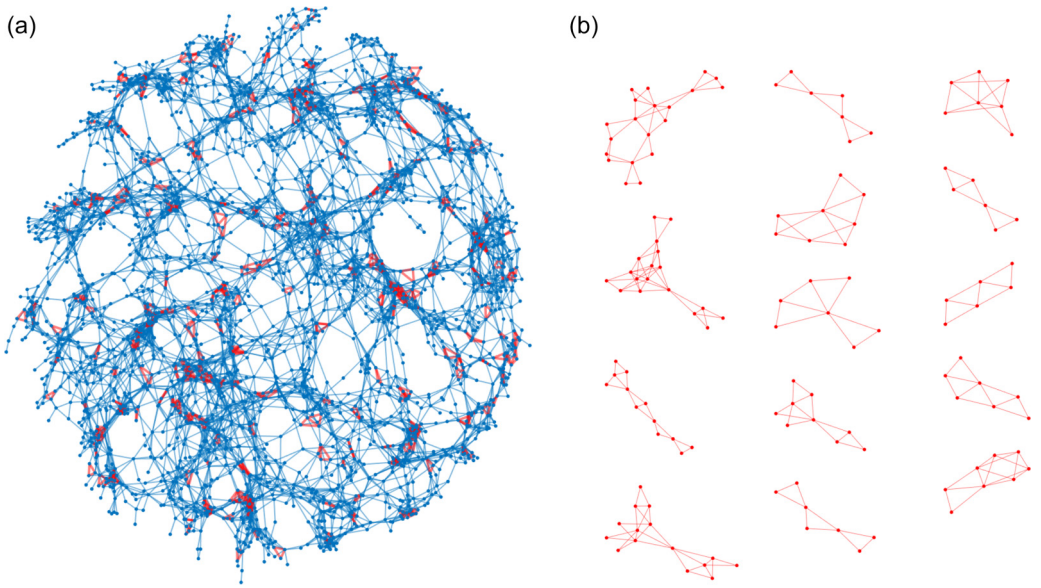

FIG. 4. (a) Hypergraph structure of a quasi-2D network of 3000 rectangles with an average connectivity of three Hopf links per rectangle, with several Borromean clusters interspersed throughout labeled in red. (b) A sample of the larger Borromean clusters appearing within the network in (a). The largest contains 20 rectangles.

mean link valence is near 3, there are roughly 1000 rectangles involved in Borromean linking, and approximately 200 Borromean clusters [Fig. 5(a)]. This suggests that, should this system be applicable to kinetoplast DNA, the biological networks likely contain a significant number of Borromean links. It is possible to use graph analysis to predict the spectrum of components released from kinetoplasts or other Olympic DNA networks as minicircles are broken with restriction enzymes [16,21], for example the number of single and double minicircles to be detected by gel electrophoresis as a function of the fraction of broken minicircles. While this model is likely too simple to make predictions for such a DNA experiment, it can estimate the hazards of ignoring Borromean connections during such a prediction. To do so, we eliminate at random matching rows and columns from the hypergraph adjacency matrix, which effectively removes a rectangle from the network and a node from the hypergraph. If the rectangle removed has Borromean connections, the adjacency values of the other two rectangles are zeroed in the matrix, effectively removing the hypergraph edges while keeping the nodes. The

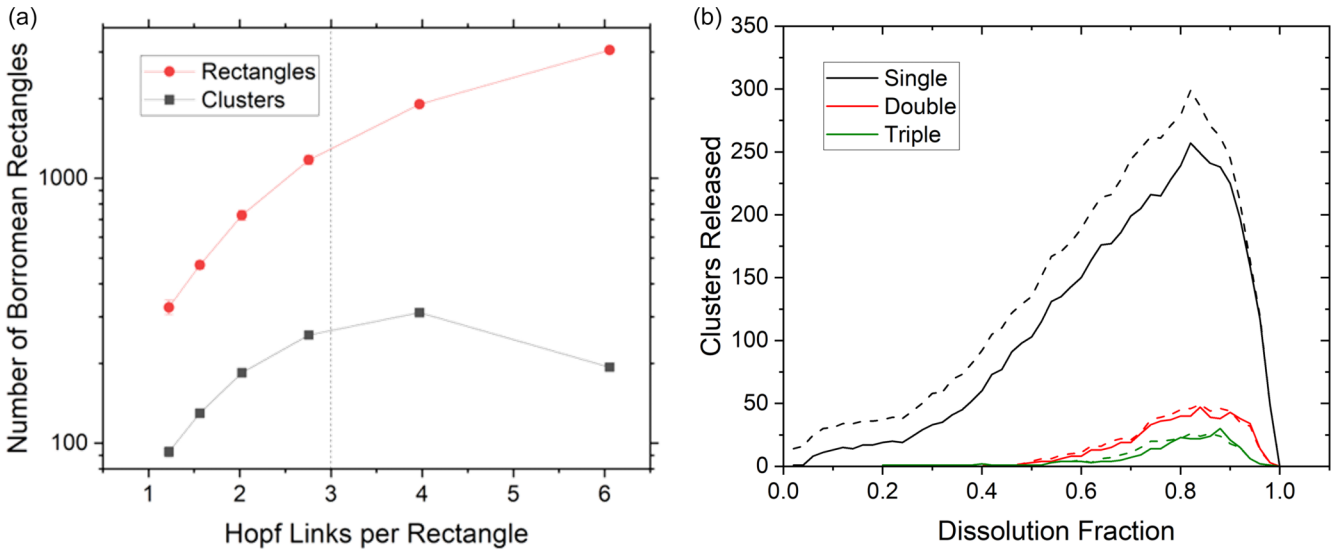

FIG. 5. (a) The number of rectangles with Borromean connections, and the total number of Borromean components, as a function of the mean number of Hopf links per rectangle. The rectangles had a uniform distribution of aspect ratios between 1.5 and 2.5 in a 5000-rectangle network confined to a disk with effective height 0.1, with an average of three Hopf connections per rectangle. (b) The number of single, double, and triple rectangles released from such a network as rectangles are removed at random. The solid lines represent the actual dissolution of the network, the dashed line shows the prediction if Borromean linking is ignored.

graph structure is then evaluated and the number of components of size 1, 2, and 3 is measured as a function of the number of rectangles removed. We can also do this with the Hopf-only adjacency matrix, which lacks information about Borromean connectivity. The results of such a dissolution simulation are shown in Fig. 5(b). The general trends match those used to predict kinetoplast dissolution experiments in the past [21], but the naive unborromated prediction tends to overpredict the number of single rectangles released from the network, as it ignores some of the connections that those rectangles share with their neighbors. Since Borromean clusters are more likely to be released as a triplet, the naive prediction at times underpredicts the number of triplets released from the network. In future analyses of kinetoplast DNA or bulk Olympic gels made from DNA [14], it may be necessary to take into account Borromean connectivity when attempting to ascertain the network topology.

Finally, we may ask whether purely Borromean clusters without shared Hopf links can arise in dense networks. By definition, this would have to occur below the Hopf link percolation threshold, far below the Borromean percolation threshold. Hopf-free Borromean links can be observed in less dense systems of rectangles, but it is a rare event even with a high aspect ratio. The largest Hopf-free Borromean cluster we observed contained five rectangles. Below the Hopf percolation threshold we also observe groups of two larger Hopf clusters held together by a Borromean triplet.

In summary, we have developed an algorithm for examining the formation of random Borromean hypergraphs in networks of dense rectangles. Our model takes advantage of the geometry of rectangles to avoid computationally difficult knot invariants. We have demonstrated the random Borromean links can form within this system, and at sufficient density will form percolating clusters within a percolating Hopf-linked cluster. This model may be extended to arbitrarily rotated rectangles, whose topological overlaps may be determined with linear algebra, and ellipses for which linking and piercing may be determined based on location, normal vector, and eccentricity. Such an extension may be more applicable to ring polymer solutions. Borromean rings are the simplest Brunnian link, in which the removal of one component dissociates the entire network. Examining denser packings for four-Brunnian, five-Brunnian, etc. clusters may reveal higher-order hypergraphs forming at even higher densities. As computation speeds improve and the application of knot invariants to physical systems becomes more developed, it may become feasible to investigate analogous random Borromean connection and percolation in entangled polymer solutions and Olympic gels. Triple threadings between polymer rings, however, may be rare compared to rectangles as the available area for piercing grows only linearly with the length of a ring polymer in a gel [23], but folded ring polymers may be more likely to form Borromean connections. Coupled to newer quantitative experimental techniques to investigate kinetoplast DNA topology, this may lead to the discovery of naturally occurring Borromean networks.

ACKNOWLEDGMENTS

This work was supported by the National Science Foundation, Grant No. 2122199. The author appreciates Davide Michieletto for providing feedback on the work. Both peer referees had insightful and constructive feedback.

APPENDIX

In the text we stated that a network of identical rectangles forms two distinct interpenetrating Borromean networks, which we will elaborate upon here. To understand why, consider two identical rectangles A and B, both in the XY plane, overlapping with the same four corner coordinates and centered on the origin. Take the rectangles to be in the landscape orientation such that their width in X is greater than their height in Y. Rotate B 90° around the z axis so that it is now portrait in the XY plane. Then, rotate it 90° around the x axis so that it is in the XZ plane. In this case, B will pierce A. Reverting to the original configuration, keep B landscape and rotate it around the x axis so that it is in the XZ plane. In this case, A and B will intersect in two places, but they will not

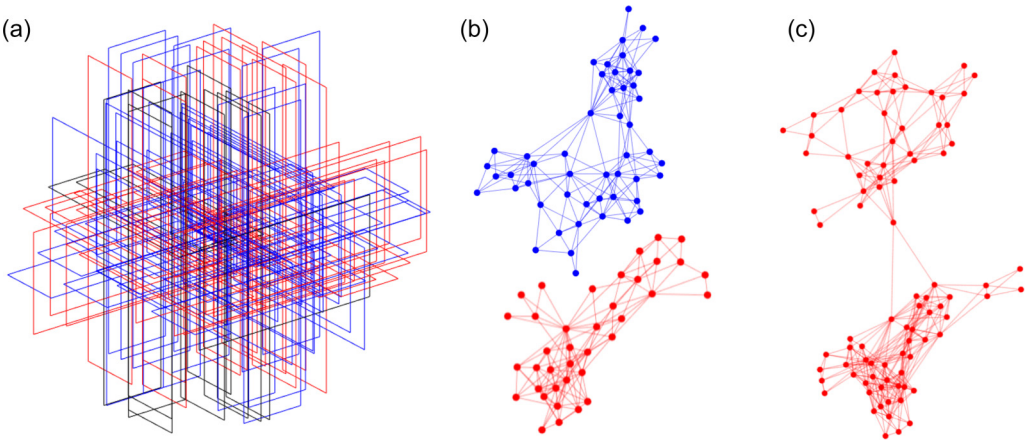

FIG. 6. (a) A network of 100 rectangles forming a single Hopf-linked network and two distinct Borromean networks, one with 50 rectangles labeled blue and the other with 38 labeled red. The twelve unborromated rectangles are black. Red and blue rectangles with the same normal vector have opposite orientations. (b) The Borromean graph structure of the network in (a). (c) Borromean graph structure of a different network in which the aspect ratio is allowed by vary uniformly by 10%. By chance, a single rectangle unites the two networks into a single Borromean cluster.

be linked or pierced. If either is translated a small distance in the x direction, they will link, but they cannot pierce in this orientation. Congruent rectangles in different planes must have compatible orientations in order to pierce each other, and the same considerations apply when a third rectangle is considered to complete the Borromean triplet. Note that if the rectangles have a different aspect ratio but the same area or perimeter, or the same aspect ratio but a different size, this does not apply.

This is visualized for a quasi-2D network of 100 rectangles in Fig. 6(a), in which rectangles from each Borromean network are colored red or blue. Note that this occurs in high-density systems in which there is a single percolating Hopf cluster, so the two subnetworks are not completely independent. Although it can be hard to parse this image by eye, the blue rectangles seen at the top of the image have the same normal vector as the red rectangles at the right of the image, but opposite orientations. The Borromean hypergraph structure is shown in Fig. 6(b); there are no shared Borromean connections between the blue and the red rectangles. If, however, the aspect ratio is allowed to vary by a small amount, it becomes possible that rectangles will be linked to both clusters, forming a single Borromean cluster throughout the system. Such an example is depicted in Fig. 6(c), in which the aspect ratio was allowed to vary by 10%. The data in Fig. 3 was taken with a fixed aspect ratio and area, but if the aspect ratio is allowed to vary then the wider rectangles will be more likely to share Borromean links, increasing the size of Borromean clusters and allowing percolation to occur at slightly lower densities.

[1] L. Tubiana, G. P. Alexander, A. Barbensi, D. Buck, J. H. E. Cartwright, M. Chwastyk, M. Cieplak, I. Coluzza, S. Čopar, D. J. Craik *et al.*, Topology in soft and biological matter, Phys. Rep. **1075**, 1 (2024).

[2] H. Watanabe, Viscoelasticity and dynamics of entangled polymers, Prog. Polym. Sci. **24**, 1253 (1999).

[3] V. P. Patil, H. Tuazon, E. Kaufman, T. Chakrabortty, D. Qin, J. Dunkel, and M. S. Bhamla, Ultrafast reversible self-assembly of living tangled matter, Science **380**, 392 (2023).

[4] A. R. Klotz, B. W. Soh, and P. S. Doyle, Equilibrium structure and deformation response of 2D kinetoplast sheets, Proc. Natl. Acad. Sci. USA **117**, 121 (2020).

[5] E. Panagiotou, K. C. Millett, and S. Lambropoulou, The linking number and the writhe of uniform random walks and polygons in confined spaces, J. Phys. A: Math. Theor. **43**, 045208 (2010).

[6] D. Michieletto and M. S. Turner, A topologically driven glass in ring polymers, Proc. Natl. Acad. Sci. USA **113**, 5195 (2016).

[7] T. C. O'Connor, T. Ge, M. Rubinstein, and G. S. Grest, Topological linking drives anomalous thickening of ring polymers in weak extensional flows, Phys. Rev. Lett. **124**, 027801 (2020).

[8] D. DeTurck, H. Gluck, R. Komendarczyk, P. Melvin, C. Shonkwiler, and D. S. Vela-Vick, Triple linking numbers, ambiguous Hopf invariants and integral formulas for three-component links, Matematica Contemporanea **34**, 251 (2009).

[9] J. Cao, J. Qin, and S. T. Milner, Simulating constraint release by watching a ring cross itself, Macromol. **47**, 2479 (2014).

[10] W. Michalke, M. Lang, S. Kreitmeier, and D. Göritz, Simulations on the number of entanglements of a polymer network using knot theory, Phys. Rev. E **64**, 012801 (2001).

[11] M. A. Ubertini and A. Rosa, Topological analysis and recovery of entanglements in polymer melts, Macromol. **56**, 3354 (2023).

[12] T. A. Shapiro and P. T. Englund, The structure and replication of kinetoplast DNA, Annu. Rev. Microbiol. **49**, 117 (1995).

[13] B. A. Krajina, A. Zhu, S. C. Heilshorn, and A. J. Spakowitz, Active DNA olympic hydrogels driven by topoisomerase activity, Phys. Rev. Lett. **121**, 148001 (2018).

[14] S. Speed, A. Atabay, Y.-H. Peng, K. Gupta, T. Müller, C. Fischer, J.-U. Sommer, M. Lang, and E. Krieg, Assembling a true 'Olympic Gel' from >16,000 combinatorial DNA rings, https://www.biorxiv.org/content/10.1101/2024.07.12.603212v1.

[15] Y. Diao, K. Hinson, R. Kaplan, M. Vazquez, and J. Arsuaga, The effects of density on the topological structure of the mitochondrial dna from trypanosomes, J. Math. Biol. **64**, 1087 (2012).

[16] D. Michieletto, D. Marenduzzo, and E. Orlandini, Is the kinetoplast dna a percolating network of linked rings at its critical point? Phys. Biol. **12**, 036001 (2015).

[17] D. G. Ferschweiler, R. Blair, and A. R. Klotz, Percolation and dissolution of Borromean networks, Phys. Rev. E **107**, 024304 (2023).

[18] G. Bianconi and S. N. Dorogovtsev, Theory of percolation on hypergraphs, Phys. Rev. E **109**, 014306 (2024).

[19] J. Hopcroft and R. Tarjan, Algorithm 447: efficient algorithms for graph manipulation, Commun. ACM **16**, 372 (1973).

[20] J. Lin and H. Chen, Measurement of continuum percolation properties of two-dimensional particulate systems comprising congruent and binary superellipses, Powder Technol. **347**, 17 (2019).

[21] J. Chen, C. A. Rauch, J. H. White, P. T. Englund, and N. R. Cozzarelli, The topology of the kinetoplast DNA network, Cell **80**, 61 (1995).

[22] P. He, A. J. Katan, L. Tubiana, C. Dekker, and D. Michieletto, Single-molecule structure and topology of kinetoplast DNA networks, Phys. Rev. X **13**, 021010 (2023).

[23] J. Smrek and A. Y. Grosberg, Minimal surfaces on unconcatenated polymer rings in melt, ACS Macro Letters **5**, 750 (2016).